

Transverse lightwave circuits in microstructured optical fibers: waveguides

Maksim Skorobogatiy

*École Polytechnique de Montréal, Génie Physique, C.P. 6079, succ. Centre-Ville Montreal,
Québec H3C3A7, Canada*

maksim.skorobogatiy@polymtl.ca

<http://www.photonics.phys.polymtl.ca>

Kunimasa Saitoh and Masanori Koshiba

Division of Media and Network Technologies, Hokkaido University, Sapporo 060-0814, Japan

Abstract: Novel class of microstructured optical fiber couplers is introduced that operates by resonant, rather than proximity, energy transfer via transverse lightguides built into a fiber cross-section. Such a design allows unlimited spatial separation between interacting fibers which, in turn, eliminates inter-core crosstalk via proximity coupling. Controllable energy transfer between fiber cores is then achieved by localized and highly directional transmission through a transverse lightguide. Main advantage of this coupling scheme is its inherent scalability as additional fiber cores could be integrated into the existing fiber cross-section simply by placing them far enough from the existing circuitry to avoid proximity crosstalk, and then making the necessary inter-core connections with transverse light “wires” - in a direct analogy with an on chip electronics integration.

© 2005 Optical Society of America

OCIS codes: 060.1810,130.3120

References and links

1. C.M. Smith, N. Venkataraman, M.T. Gallagher, D. Muller, J.A. West, N.F. Borrelli, D.C. Allan, K.W. Koch, “Low-loss hollow-core silica/air photonic bandgap fibre,” *Nature* **424**, 657-659 (2003).
2. P. Russell, “Photonic crystal fibers,” *Science* **299**, 358-362 (2003).
3. M.A. van Eijkelenborg, A. Argyros, G. Barton, I.M. Bassett, M. Fellow, G. Henry, N.A. Issa, M.C.J. Large, S. Manos, W. Padden, L. Poladian, J. Zagari, “Recent progress in microstructured polymer optical fibre fabrication and characterisation,” *Opt. Fiber Techn.* **9**, 199-209 (2003).
4. B. Temelkuran, S.D. Hart, G. Benoit, J.D. Joannopoulos, Y. Fink, “Wavelength-scalable hollow optical fibres with large photonic bandgaps for CO₂ laser transmission,” *Nature* **420**, 650-653 (2002).
5. T. Katagiri, Y. Matsuura, M. Miyagi, “Photonic bandgap fiber with a silica core and multilayer dielectric cladding,” *Opt. Lett.* **29**, 557-559 (2004).
6. B.J. Mangan, J.C. Knight, T.A. Birks, P.St.J. Russell, and A.H. Greenaway, “Experimental study of dual-core photonic crystal fibre,” *Electron. Lett.* **36**, 1358-1359 (2000).
7. B.H. Lee, J.B. Eom, J. Kim, D.S. Moon, U.-C. Paek, and G.-H. Yang, “Photonic crystal fiber coupler,” *Opt. Lett.* **27**, 812-814 (2002).
8. W.E.P. Padden, M.A. van Eijkelenborg, A. Argyros, N. A. Issa, “Coupling in a twin-core microstructured polymer optical fiber,” *Appl. Phys. Lett.* **84**, 1689-1691 (2004).
9. H. Kim, J. Kim, U.-C. Paek, B.H. Lee, and K. T. Kim, “Tunable photonic crystal fiber coupler based on a side-polishing technique,” *Opt. Lett.* **29**, 1194-1196 (2004).

10. J. Laegsgaard, O. Bang, and A. Bjarklev, "Photonic crystal fiber design for broadband directional coupling," *Opt. Lett.* **29**, 2473-2475 (2004).
 11. K. Saitoh and M. Koshiba, "Leakage loss and group velocity dispersion in air-core photonic bandgap fibers," *Opt. Express* **11**, 3100 (2003). <http://www.opticsexpress.org/abstract.cfm?URI=OPEX-11-23-3100>
 12. K. Saitoh, M. Koshiba, "Full-vectorial imaginary-distance beam propagation method based on a finite element scheme: application to photonic crystal fibers," *J. Quantum Electron.* **38**, 927-933 (2002).
 13. K. Saitoh, M. Koshiba, "Full-vectorial imaginary-distance beam propagation method with perfectly matched layers for anisotropic optical waveguides," *J. Lightwave Technol.* **19**, 405-413 (2001).
 14. M. Skorobogatiy, "Modeling the impact of imperfections in high-index-contrast photonic waveguides," *Phys. Rev. E* **70**, 46609 (2004).
 15. M. Skorobogatiy, "Hollow Bragg fiber bundles: when coupling helps and when it hurts," *Opt. Lett.* **29**, 1479-1481 (2004).
-

1. Introduction

Currently, one of the major trends in the development of all-fiber devices is an increasing integration of functionalities in a single fiber. The ultimate goal is to be able to fabricate in a single draw a complete all fiber component provisioned on a preform level. Some of the advantages of all-fiber devices are: simplified packaging, absence of sub-component splicing losses, environmental stability due to the absence of a free space optics. While the benefits of integrated all-fiber devices are significant enough to encourage development of increasingly complex components, the major roadblock to their realization is an unavoidable complexity of the required transverse refractive index profile. From an experimental point of view, complex preform geometries such as in microstructured optical fibers (MOF) [1, 2, 3], and multicomponent material combinations such as in Bragg fibers [4, 5] result in major challenges for the preform fabrication and drawing. Assuming that these technological issues could be resolved there is still a conceptual difficulty in the implementation of increasingly complex fiber profiles. Namely, many of the interesting functionalities that fiber devices offer such as modal dispersion profile design, directional power transfer between several fiber cores [6, 7, 8, 9, 10], inter-mode conversion, etc. rely critically on proximity interaction between the modes localized in different spatial regions. Requirement of a finite overlap between the interacting modes, typically, forces multi-core systems to be designed to operate on a principle of proximity interaction, where different cores are placed in an immediate proximity of each other. Such arrangement forms an all-interacting system where all the fibers have to be considered simultaneously with a complexity of a system design increasing dramatically with the number of fiber cores. While it can be beneficial to have the individual sub-components designed on a proximity principle, scalable integration of several of them in a single fiber would rather require the individual spatially separated "non-interacting" sub-components connected by a "wire"-like transverse lightwave circuitry. In this paper we will demonstrate the principles of design of such transverse lightguides enabling long range energy transfer between the two widely separated cores.

2. Structure and definitions

In this paper, we review a "work-horse" of the fiber components - a directional coupler. In its traditional implementation two fiber cores are placed in a close proximity of each other. Inter-core coupling is due to a finite overlap between the corresponding core modes leading to a complete energy transfer from one core into the other after a certain "coupling" length L_c . By choosing the overall coupler length to be finite and equal to L_c directionality of energy transfer is achieved. When two cores are spaced further apart an inter-core coupling reduces dramatically resulting in an exponential increase of a coupling length. In what follows we demonstrate designing of a resonant rather than a proximity coupler which enables energy transfer between the two fiber cores regardless of the inter-core separation. To demonstrate robustness of our

design and to investigate an importance of the bandgap confinement on the coupler radiation losses we choose the most challenging case - designing of a long range coupling between the two hollow core fibers guiding in the band gap of a surrounding 2D photonic crystal cladding. Structure and modal properties of the individual hollow waveguides are detailed in [11]. Briefly, hollow core is formed in a silica based MOF with a cladding refractive index $n = 1.45$ by removing two rows of tubes and smoothing the resulting core edges. The pitch is $\Lambda = 2\mu\text{m}$, while $d/\Lambda = 0.9$ with a total of six hole layers in the cladding. Fundamental band gap where the core guided modes are found extends between $1.29\mu\text{m} < \lambda < 1.40\mu\text{m}$. To form a coupler we place two hollow cores N periods apart from each other as shown in Fig. 1. Transverse waveguide is then introduced by slightly reducing (high index defect) or increasing (low index defect) the diameters of the holes along the line joining the cores. As hollow core size is relatively small, in order to minimize the impact on the guided modes of a single fiber we keep the sizes of the holes closest to the cores unchanged. In a stand alone fiber the lowest loss mode is a doublet

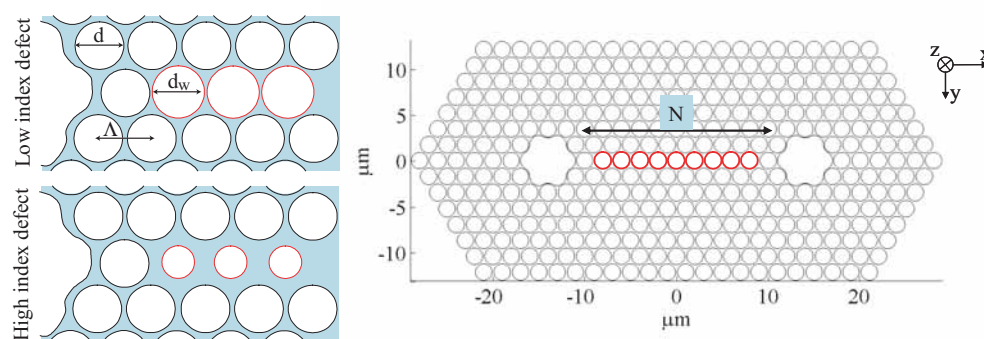


Fig. 1. Schematic of a two hollow core MOF coupler. Cores are separated by N lattice periods. Transverse waveguide is formed by the holes of somewhat different diameters placed along the inter-core line. Holes closest to the cores are not modified.

with an electric field vector having either x or y dominant component. We call such fields as x or y polarized. In what follows we consider each polarization separately, making all the derivations only for a y polarized mode. When second identical core is introduced, interaction between the core modes of the same polarization leads to an appearance of the even and odd (with respect to the reflection in OY axis) supermodes with the effective refractive indexes defined respectively as n_{eff}^{y+} , n_{eff}^{y-} closely spaced around n_0^y of a single core fiber mode. An inter-fiber coupling strength is then defined by difference in the real parts of the supermode effective indexes $\Delta n_{eff}^y = |Re(n_{eff}^{y+} - n_{eff}^{y-})|$, while modal radiation losses are defined by the imaginary parts of their effective indexes. Coupling length after which the power launched in one core will be completely transferred into the other is $L_c = \lambda / (2\Delta n_{eff}^y)$. To find an upper bound on the radiation losses of a coupler we define the power decay length as $L_d = \lambda / (4\pi \max(Im(n_{eff}^{y\pm})))$. Maximum power loss over a single coupling length is then $P(L_c)/P(0) = \exp(-L_c/L_d)$. In what follows, we use the FEM mode solver [12] to perform modal analysis of a coupler as well as the FEM BPM solver [13] to confirm our findings.

3. Proximity coupling between two hollow cores

We first investigate proximity coupling between two hollow cores without any line defects in the cladding. In Fig. 2(a) dispersion relations of the y even and odd supermodes of a two core

coupler with $N = 4$ are presented with respect to a dispersion relation of a y polarized mode of a stand alone fiber; modal splitting due to the proximity coupling is evident. In the inset, $|E_y|$ field distribution of one of the supermodes is presented. Due to exponentially small field presence in the cladding, plots of absolute field values will look very much the same for both supermodes. Coupling length for $N = 4$ varies between $3 - 8\text{cm}$ achieving its maximum value well inside of a band gap where modal confinement in the core is strongest. Although inter-core coupling increases near the band gap edges as core mode becomes less well confined by a PBG cladding, coupler losses increase at a much faster rate, thus resulting in the dramatic increase of a coupler loss per coupling length $P(L_c)/P(0)$ when approaching the band gap edges.

In Fig. 2(a) note that effective index curves of the two supermodes are not centered around the effective index curve of an unperturbed mode as predicted by a standard perturbation theory (PT). We have observed the same failure of a standard PT even when inter-core separation is increased beyond 11 periods and mode coupling becomes negligibly small. This failure is a vivid example of a general observation that predictions of a standard PT are generally not applicable to the high index-contrast systems with shifting material boundaries (see [14] and the references of thereof). Another example of a high index-contrast coupler with a similar anomaly in the behavior of its supermodes is a case of two coupled hollow Bragg fibers detailed in [15]. As the fields of the core modes guided by PBG decay exponentially fast into the cladding,

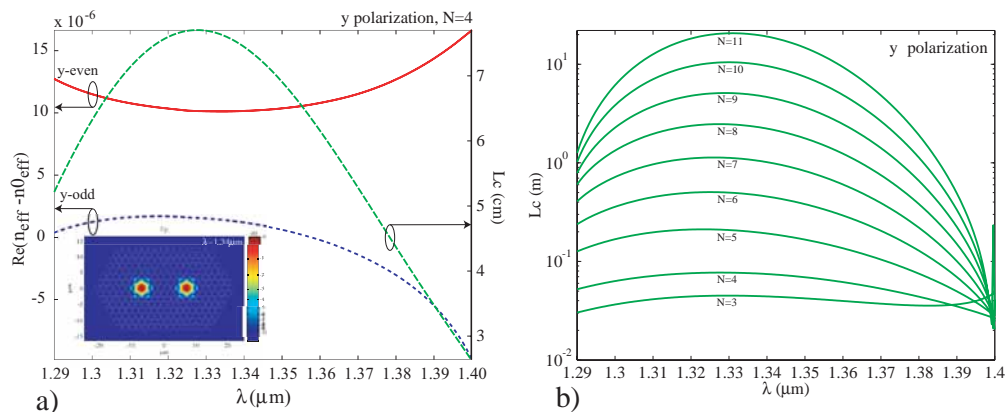


Fig. 2. a) Proximity coupling between the modes of two cores separated by 4 periods, dispersion relations, coupling length. b) Proximity coupling length as a function of λ for various inter-core separations.

coupling between the cores also decreases exponentially fast when separation between the cores is increased. In Fig. 2(b) we clearly observe this trend by plotting on a log scale coupling length across the band gap for the various inter-core separations N . Thus, for an inter-core separation $N = 4$ coupling length is $\sim 10\text{cm}$, for $N = 7$ it is $\sim 1\text{m}$, while for $N = 11$ it is $\sim 20\text{m}$. In what follows we will demonstrate that introduction of the transverse waveguides enables reduction of a coupling length to a sub centimeter scale even for large separations $N = 11$ making such a resonant coupling practically independent of an inter-core separation.

4. Resonant coupling between two hollow cores

We now introduce the high index line defect (transverse waveguide) into the $N = 4$ coupler of Fig. 2(a) by reducing inner diameters of all the holes along the inter-core line to $d_w/\Lambda = 0.85$. In the upper plot of Fig. 3(a) dispersion relation of the supermodes relative to the dispersion relation of a fundamental mode of an isolated core is presented. At $\lambda \sim 1.305\mu\text{m}$, $y - \text{even}$

supermode experiences avoiding crossing with a localized state of a line defect. In this regime there are three modes interacting: y -odd mode (point 2 in Fig. 3(a)), and two y -even modes (points 1,3 in Fig. 3(a)). Field distribution in a y -odd mode is similar to that of a Fig. 2(a). Field distributions in the y -even supermodes reflect properly symmetrized linear combinations of the individual core modes and a line defect mode (see Fig. 3(b)); due to a small field overlap between the core modes and a line defect mode, plots of absolute field values appear similar for both supermodes. When three modes interact, complete power transfer between the cores is

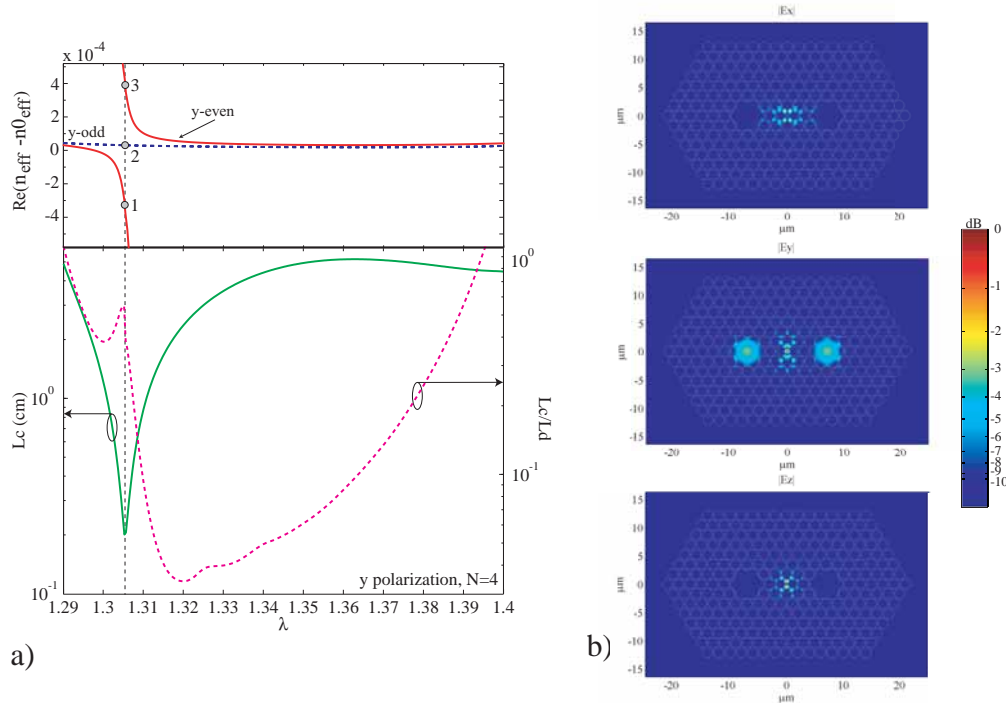


Fig. 3. Resonant coupling between the modes of two cores separated by 4 periods mediated by a line defect. a) Upper plot: dispersion relations of the supermodes exhibiting avoiding crossing with the transverse waveguide modes. Lower plot: coupling length, losses. b) Field distribution of a y -even supermode at $\lambda = 1.3052\mu\text{m}$ resonance. Excitation of a localized mode of a line defect is observed in an inter-core region.

still possible with the same definition of coupling length as in section 2, given that the distance between points 1 and 2 is the same as the one between 2 and 3. In what follows we call this a resonance. In the lower plot of Fig. 3(a) we present coupling length across the band gap (solid curve), using as coupling strength $\Delta n_{\text{eff}}^y = \min(|\text{Re}(n_{\text{eff}}^{y_1+} - n_{\text{eff}}^{y-}|), |\text{Re}(n_{\text{eff}}^{y_2+} - n_{\text{eff}}^{y-odd}|)$), which at the resonances gives coupling length for a complete energy transfer. At $\lambda = 1.3052\mu\text{m}$ coupling length becomes as small as $L_c = 2\text{mm}$, while far from the point of resonance, two mode interaction picture becomes valid again and coupling length becomes similar to that of a proximity interaction. Another important characteristic of a resonant coupler is the radiation loss over a single coupling length. In section 2 we estimated an upper bound for such a loss to be $1 - P(L_c)/P(0) = 1 - \exp(-L_c/L_d)$, which in the limit of a small coupling loss becomes simply L_c/L_d . In Fig. 3(a) L_c/L_d parameter is presented across the band gap. At resonance, the coupling loss exhibits large increase, while outside a resonance in the region dominated by

proximity coupling, radiation loss follows a general trend to be the smallest inside of a band gap while increasing towards the band gap edges. In this particular example an upper bound estimate gives a $-2.4dB$ loss per coupling length. For a system with a line defect, while at resonance, there is a substantial power transfer to a strongly localized state of a transverse waveguide (in the perpendicular to a fiber direction). As dispersion relation of a supermode is close to that of an air line, confinement in a higher refractive index line defect is only possible by the band gap of a cladding. Thus, if the cladding were infinite, radiation losses of a defect state would be zero. To understand better the origin of the radiation losses when coupling via a transverse line defect it is useful to think about such a line defect in a limit of an infinite transverse waveguide connecting two infinitely separated fiber cores. Such system will exhibit a discrete translational symmetry along the direction of a transverse waveguide having well defined guided states. In the case of a finite cladding, losses of the line defect modes will be ultimately determined by their location in the band gap of a cladding - the deeper into the band gap the lower would be the losses. When creating a transverse waveguide by reducing the sizes of all the holes along a certain direction, one "pulls" into the band gap of a cladding a defect state associated with a transverse waveguide. Thus, the larger (up to a certain extent) is a change in the hole sizes the deeper into the band gap of a cladding will the guided modes of a line defect be located, consequently leading to the lower losses of the transversely guided modes of a line defect.

We now increase the number of periods between the cores to $N = 11$. If there were no transverse waveguide connecting the cores proximity coupling would be very small resulting in a very large coupling length of $L_c \sim 20m$. In the upper plot of Fig. 4(a) dispersion relation of the supermodes relative to the dispersion relation of a fundamental mode of an isolated core is presented for a line defect of $d_w/\Lambda = 0.85$. As distance between the cores increases, several resonances appear inside of the band gap. These states are associated with the points of avoiding crossing of the dispersion relation of a fundamental mode of a hollow core with the dispersion relations of the transversely guided modes of a line defect (which in the limit of infinite inter-core separation becomes a true transverse waveguide). Excitation of the transversely guided modes of a transverse waveguide is possible as hollow core guided mode has a considerable transverse wavevector component in a PBG cladding. Coupling lengths at resonances become very small and on the order of the few millimeters (see Fig. 4(a) lower plot). Long range coupling and complete power transfer at resonances have been confirmed with beam propagation method (BPM) simulations. In the lower plot of Fig. 4 results of BPM simulations for the coupling length, as well as the loss over a single coupling length are presented as solid curves with circles, exhibiting excellent agreement with the predictions of a modal analysis. At the resonances complete power transfer over a single coupling length is observed between the cores, while out of the resonances only a partial power transfer is observed. In the media file, results of a BPM simulation of a power transfer between the two hollow cores at the $\lambda = 1.30639\mu m$ resonance is demonstrated over the propagation distance of ten coupling lengths confirming our modal analysis predictions. At $\lambda \sim 1.306\mu m$, a $y - even$ supermode exhibits avoiding crossing with a localized line defect state. In this regime there are three modes interacting: $y - odd$ mode (point 2 in Fig. 4(a)), and two $y - even$ modes (points 1,3 in Fig. 4(a)). Field distribution in a $y - odd$ mode is similar to that of Fig. 2(a), while field distribution in the $y - even$ modes exhibits a strong mixing with a line defect mode Fig. 4(b).

In Fig. 5 at four consecutive resonances we present the amplitude distributions of the y components of the electric fields in the supermodes strongly mixed with the transverse guided modes of a line defect. Standing wave pattern in the inter-core region arises due to the excitations of both forward and backward propagation modes in a transverse waveguide. Also, toward shorter wavelengths the number of the spatial oscillations in the defect region increases. In this respect, the modes of a line defect are analogous to the Fabry-Perot resonances excited in a

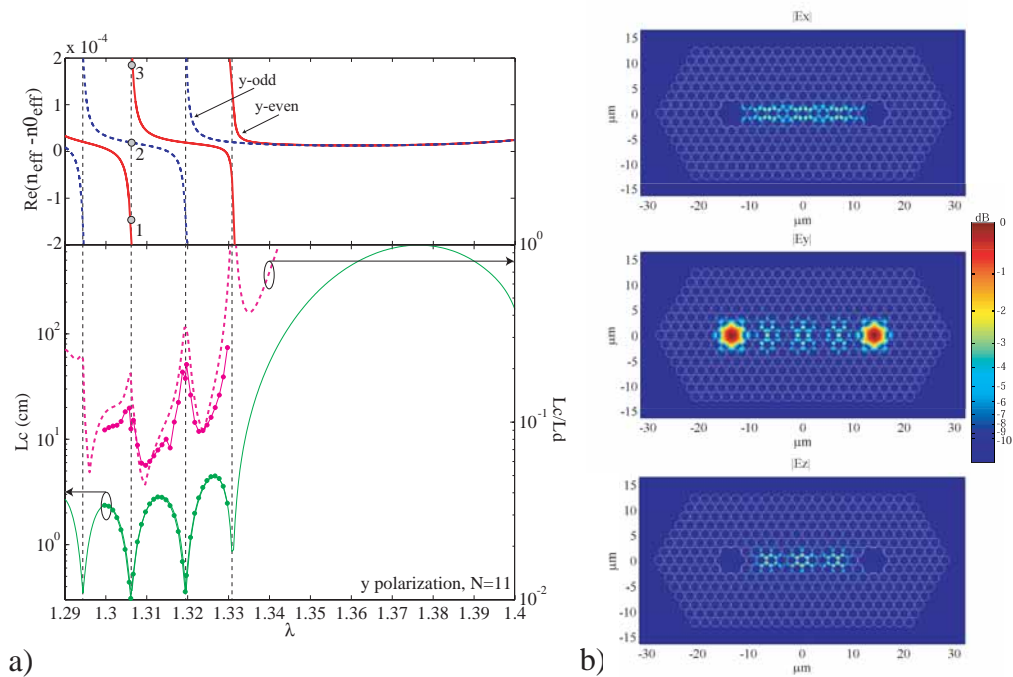


Fig. 4. Resonant coupling between the modes of two cores separated by 11 periods mediated by a line defect. a) Upper plot: dispersion relations of the supermodes exhibit avoiding crossing with waveguide modes. Lower plot: coupling length from the modal analysis (solid) and BPM (solid with circles), losses from the modal analysis (dashed) and BPM (dashed with circles). b) Field distribution of a y -even supermode at the $\lambda = 1.3064\mu\text{m}$ resonance. Excitation of a localized line defect mode is observed in the inter-core region.

short transverse waveguide terminated by the hollow cores. Origin of the localized Fabry-Perot states in the inter-core region can be understood from a simplified interaction model. Particularly, we consider coupling in our system to be analogous to the coupling between the core guided modes of the two collinear fibers via the in-plane guided modes of a slab waveguide; fiber center lines are assumed to be in the plane of a slab. Modes of a slab waveguide are degenerate with respect to a travelling direction along the waveguide plane. At a given frequency ω we define a propagation constant of a guided slab state as $k(\omega)$ with a direction of propagation anywhere in the plane of a slab. Now assume that a guided fiber mode is characterized by an in-plane propagation vector $(\beta, 0)$, where OX axis is along the fiber propagation direction, and OY axis is perpendicular to the fiber and is in the plane of a slab waveguide. For a given frequency ω guided fiber mode will be phase matched with two modes of a slab waveguide with the propagation vectors $(\beta, \pm k_t)$, where the transverse propagation constant is defined as $k_t = \sqrt{k(\omega)^2 - \beta^2}$. If k_t is real, guided slab modes will form a standing wave (Fabry-Perot resonance) whenever constructive interference condition is satisfied $k_t L \sim \pi p$, where L is a distance between the fibers and p is an integer. As inter-core distance is increased more resonances will appear in the inter-core region with spectral separation between the resonances being inversely proportional to an inter-core separation. In a hollow core MOF coupler $\beta \sim \omega$, $k(\omega) \sim n_{\text{clad}}\omega$, thus for an inter-core separation of $N\Lambda$ spectral separation between the reso-

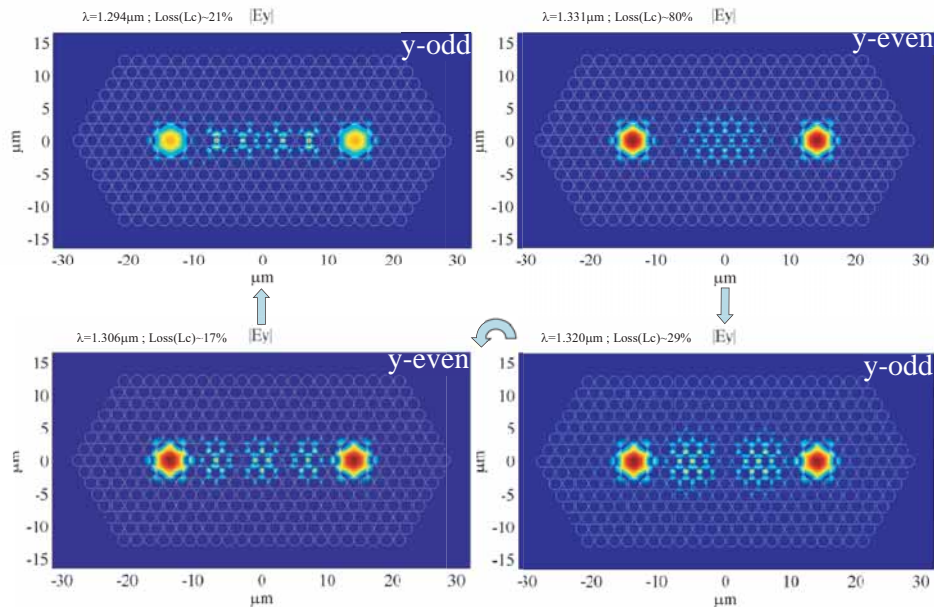


Fig. 5. Field distribution of the supermodes at the consecutive resonances for $N = 11$. The number of spatial oscillations in the inter-core region increases towards shorter wavelengths signifying Fabry-Perot nature of the localized states in a transverse waveguide.

nances will be $\Delta\lambda \sim \lambda^2 / (2N\Lambda\sqrt{n_{clad}^2 - 1})$. In Fig. 6 (right plot) coupling length as a function of the inter-core separation is presented across the band gap for a line defect $d_w/\Lambda = 0.85$. One can clearly see an appearance of Fabry-Perot resonances with reducing spectral separation between them as the inter-core distance is increased. At resonances coupling length is on the order of several millimeters regardless of the inter-core separation Fig. 6 (left plot). Note that all the resonances are located in the region $\lambda \lesssim 1.34\mu\text{m}$ suggesting that transverse guided modes of a high index line defect are pulled down from the upper edge of a band gap. Towards longer wavelengths, coupling becomes dominated by the proximity effects as there are no line defect states available at the lower frequencies.

Finally, we would like to address polarization dependence of a resonance coupler described in this work. In Figs. 7(a,b) coupling length for a high index defect $d_w/\Lambda = 0.85$ is presented. As inter fiber separation increases, y polarized resonant states of a transverse waveguide are pulled down from the upper band gap edge (shorter wavelengths), while no resonant states exist for x polarization. In Figs. 7(c,d) coupling length for a low index defect $d_w/\Lambda = 0.95$ is presented. As inter fiber separation increases, resonant states of a transverse waveguide exist for both y and x polarization and they are pulled up from the lower band gap edge (longer wavelengths). We believe that design of polarization independent long range coupler is possible by a proper choice of a line defect geometry. Our simulations suggest that low index defects are the prime candidates for polarization independent performance; work in this direction is currently underway.

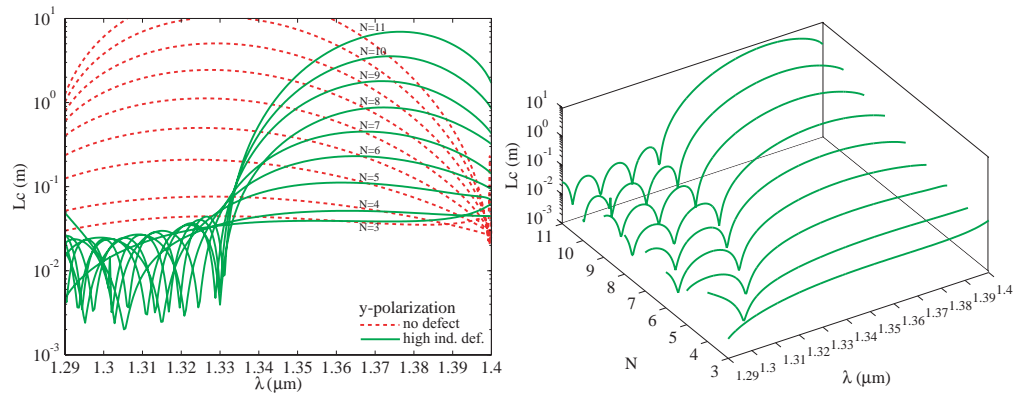


Fig. 6. Coupling length across the band gap as a function of the inter-core separation N . Left: at resonances coupling length is on the order of several millimeters regardless of the inter-core separation, at longer wavelength coupling is dominated by the proximity interaction. Right: Fabry-Perot like resonances. Spectral separation between the resonances decreases with an increasing inter-core distance.

5. Conclusions

Novel class of microstructured optical fiber couplers is introduced that operates by resonant, rather than proximity energy transfer via the transverse line defects introduced between the fiber cores. Introduction of such transverse waveguides enables significant spatial separation between the interacting fibers which, in turn, eliminates an inter-core crosstalk via the proximity coupling and allows a scalable integration of the multiple fiber sub-components. Controllable energy transfer between the cores is then achieved over a coupling length of several millimeters regardless of the inter-core separation. Findings based on the modal analysis were confirmed by the BPM simulations. Polarization independent coupler is believed to be possible based on the low index line defect design.

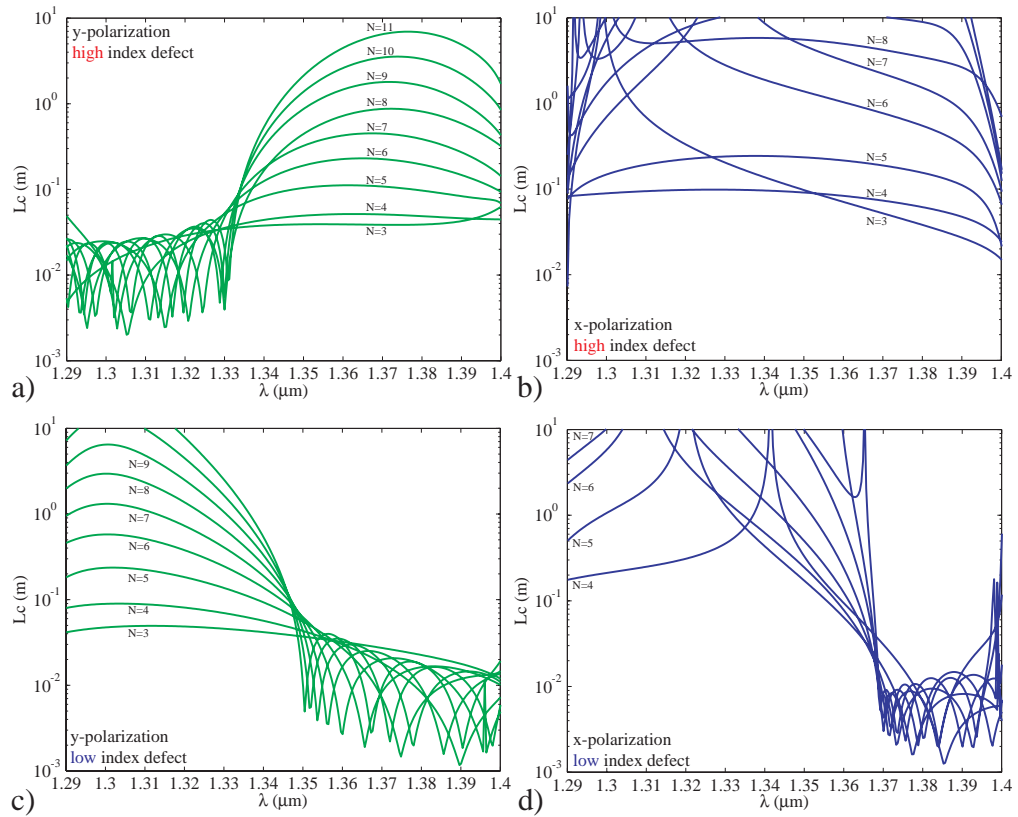


Fig. 7. Coupling length across the band gap as a function of the line defect length N , mode polarization and defect type.